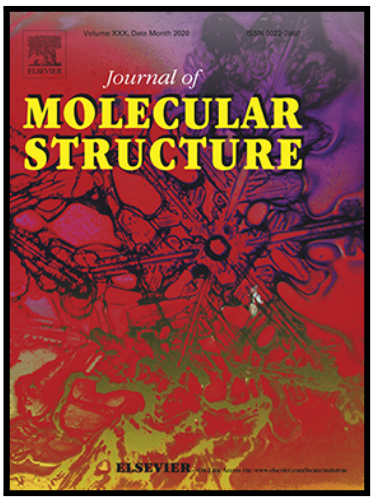

Synthesis, structural properties, enzyme inhibition and molecular docking studies of (Z)-N'-(1-allyl-2-oxoindolin-3-ylidene) methanesulfono-hydrazide and (Z)-N'-(1-allyl-2-oxoindolin-3-ylidene)-3-nitrobenzenesulfono-hydrazide

Muhammad Arshad , Kainat Ahmed , Zafar Iqbal , Umer Rashid , Muhammad Nadeem Arshad , Abdullah M. Asiri , Tariq Mahmood

PII: S0022-2860(20)31205-9
DOI: https://doi.org/10.1016/j.molstruc.2020.128880
Reference: MOLSTR 128880

To appear in: *Journal of Molecular Structure*

Received date: 23 March 2020
Revised date: 8 July 2020
Accepted date: 9 July 2020

Please cite this article as: Muhammad Arshad , Kainat Ahmed , Zafar Iqbal , Umer Rashid , Muhammad Nadeem Arshad , Abdullah M. Asiri , Tariq Mahmood , Synthesis, structural properties, enzyme inhibition and molecular docking studies of (Z)-N'-(1-allyl-2-oxoindolin-3-ylidene) methanesulfono-hydrazide and (Z)-N'-(1-allyl-2-oxoindolin-3-ylidene)-3-nitrobenzenesulfono-hydrazide, *Journal of Molecular Structure* (2020), doi: https://doi.org/10.1016/j.molstruc.2020.128880

Highlights

(i) Synthesis of two allylisatin based sulfonyl hydrazides is performed.

(ii) X-ray results are in strong correlation with the DFT studies.

(iii) Both are tested *in vitro* against *Bacillus pasteurii* urease.

(iv) Molecular docking studies further proved the mechanism of enzyme inhibition

Synthesis, structural properties, enzyme inhibition and molecular docking studies of (Z)-*N′*-(1-allyl-2-oxoindolin-3-ylidene)methanesulfono-hydrazide and (Z)-*N′*-(1-allyl-2-oxoindolin-3-ylidene)-3-nitrobenzenesulfono-hydrazide

Muhammad Arshad[a] , Kainat Ahmed[a], Zafar Iqbal[b], Umer Rashid[b], Muhammad Nadeem Arshad[c,d], Abdullah M. Asiri[c,d], Tariq Mahmood[b*]

[a]Institute of Chemistry, University of the Punjab, Quaid-i-Azam Campus, Lahore-54590, Pakistan.

[b]Department of Chemistry, COMSATS University, Abbottabad Campus, University Road, Tobe Camp, Abbottabad-22060, Pakistan.

[c]Chemistry Department, Faculty of Science, King Abdulaziz University, P. O. Box 80203, Jeddah 21589, Saudi Arabia.

[d]Centre of Excellence for Advanced Materials Research (CEAMR), King Abdulaziz University, P. O. Box 80203, Jeddah 21589, Saudi Arabia.

*To whom correspondence should be addressed: E-mail: mahmood@cuiatd.edu.pk (T.M.)

Graphical Abstract

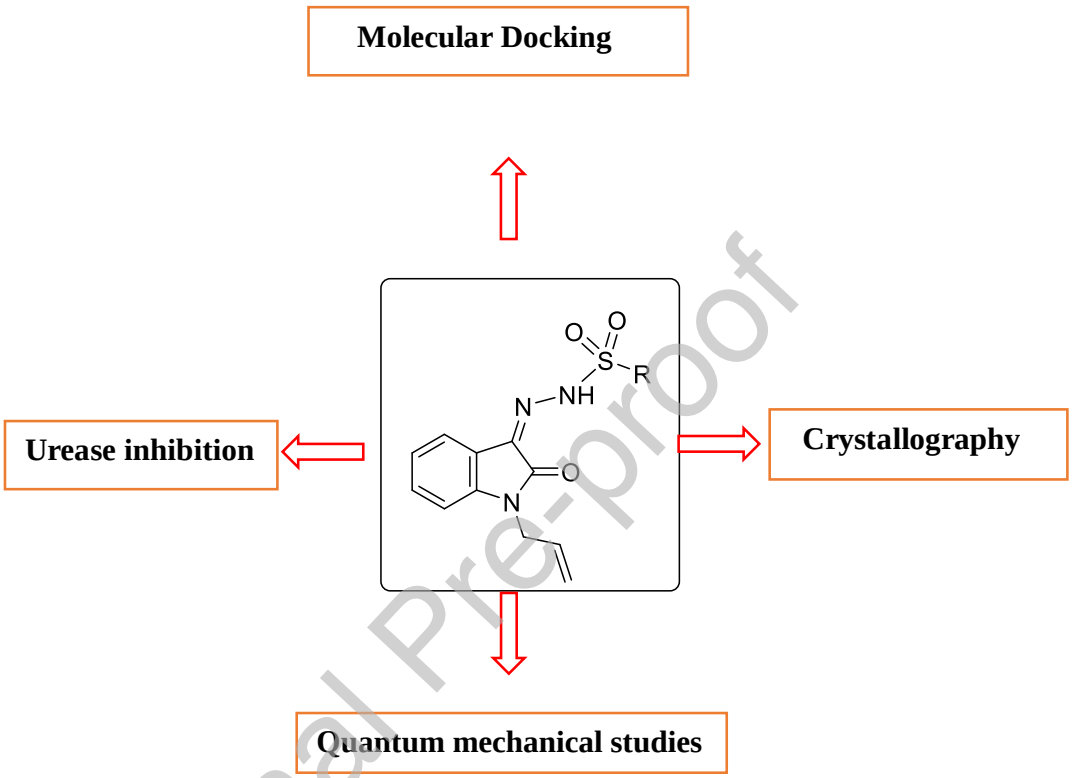

Abstract

Isatin and its derivatives exhibit broad range of biological and pharmacological applications. Keeping in view the importance of isatin and its derivatives, herein we report two isatin based new sulfono-hydrazides **4** & **5**, synthesized in high yields and characterized by spectroscopic techniques. Their structures are confirmed unequivocally using X-ray diffraction crystallography,

which revealed the presence of $P2_1/c$ (**4**) and $P2_1/n$ (**5**) space groups and unit cells stabilized through noncovalent interactions. Further details about geometric and electronic properties of compounds **4** and **5** are obtained by quantum mechanical approach based on density functional theory (DFT). These compounds are also evaluated for *in vitro* urease enzyme inhibition potential against *Bacillus pasteurii*. Both compounds inhibited the urease activity in µM concentration, however, compound **4** with IC_{50} value of 15.26 ± 0.16 µM proved to be more potent than the standard thiourea having IC_{50} value of 21.25±0.15 µM. The higher inhibition activity of compound **4** might be associated with its stronger interaction as observed by *in silico* molecular docking studies using MOE, which showed that compound **4** interacts more closely to the binding site of enzyme (4UBP) *via* Ni^{2+} ions coordination as compared to its counterpart.

Keywords: Enzyme inhibition; Isatin; Molecular docking; X-ray; DFT

1 INTRODUCTION

Isatin is a versatile heterocyclic scaffold with substantial significance for the synthesis of broad range of biologically and pharmacologically attractive motifs. Since the commercial availability of isatin in 1840 [1,2], it has been considered as synthetic for 140 years until the discovery of its natural resources. Isatin has been employed as a valuable precursor for a plethora of heterocyclic

compounds, a number of which led to the construction of medicinally important building blocks [1,3]. Over the time, isatin derivatives have been evaluated for several biological implications including antimicrobial [4], antiangiogenic [5], antitubercular [6], anxiolytic [7], and anticonvulsant agents [8]. Enzyme inhibition activity of isatin derivatives led to the discovery of tyrosine kinase inhibitors (TKI) such as Sunitinib (approved by FDA in 2006) and Nintedanib. These TKI are in clinical use for chemotherapeutic treatment of metastatic renal and gastrointestinal stroma [9] and lung cancer [10].

Enzyme inhibition is an active area of medicinal chemistry where investigations have driven towards the discovery of useful drugs against many diseases [11–13]. Urease enzyme catalyzes the hydrolysis of urea into ammonium and carbamate ions, which eventually decompose into ammonia and carbon dioxide [14,15]. The unusual rise of ammonia increases the blood pH whereupon originating a number physiological complications such as urinary catheter encrustation, gastric and peptic ulcers, hepatic coma urolithiasis and pyelonephritis [16,17]. Therefore, urease inhibitors are considered as effective remedies for controlling the damaging effect of ureolytic bacterial infections, a very common problem in developed countries [18,19]. To cater the enzymatic activity, a number of urease inhibitors including oxadiazoles [16], hydroxamic acid derivatives [20], triazoles [21], coumarins [22], piperidines [23], urea and isatin derivatives [24] have been developed, however, the quest for most potent urease inhibitors still exists.

In continuation to our efforts in the field of urease inhibition [24–26], herein, we report the synthesis, structural properties, urease inhibition and molecular docking studies of the two new allylisatin based sulfono-hydrazide derivatives.

2. Materials and Methods

2.1 Experimental

Chemicals purchased from sigma Aldrich are used further without any purification. All solvents are distilled and dried before using in chemical reactions. Melting points of both compounds are uncorrected and measured by using digital melting point apparatus (range is up to 300 ^{o}C). Absorption spectra of both derivatives are scanned by using t80 + UV/Vis spectrophotometer. Vibrational spectra (FT-IR) are monitored by using Agilent FT-IR Cary 630 instrument, using ATR sampling method. ^{1}H and ^{13}C-NMR spectra are recorded using deuterated chloroform ($CDCl_3$) as NMR solvent on Bruker's 400 MHz NMR machine.

2.2 Synthesis

The synthesis of both compounds is accomplished starting form commercially available isatin. For entire synthetic scheme see the Fig. 1.

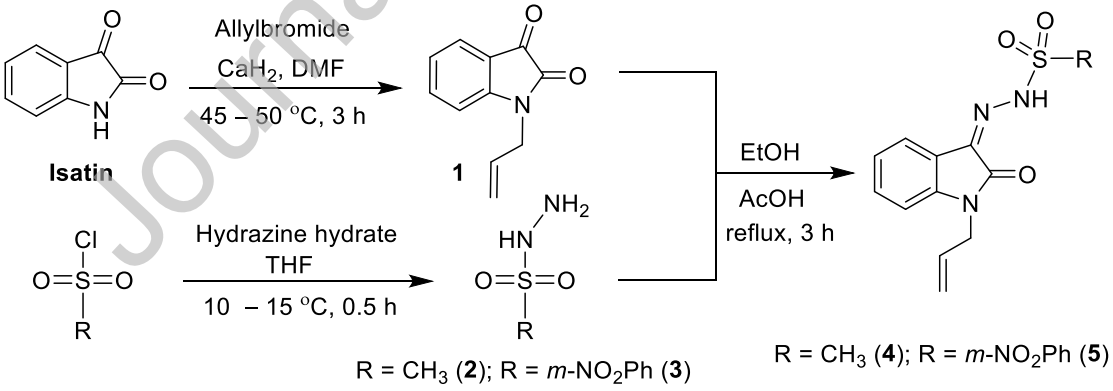

Fig.1; Synthesis of *N*-allylisatin derived sulfono-hydrazides **(4** & **5)**

2.2.1 N-allylation of isatin

Isatin (1.47 g, 10 mmol) in DMF (20 ml) was taken in round bottom flask. Calcium hydride (0.63 g, 15 mmol) added to the reaction mixture and heated at 50 ^{o}C for 30 minutes. Allylbromide (1.81 g, 15 mmol) was added and stirred the mixture for 3 hours at 45–50 ^{o}C. Upon completion as indicated by TLC, ice cold water (100 ml) was added for precipitation of required product. The precipitates were filtered, washed with water, dried in air and further purified by recrystallization from ethanol to obtain compound **1** as reddish crystalline solid (1.46 g, 78%).

*2.2.2 Synthesis of sulfonyl hydrazides (**2** and **3**)*

Both intermediate compounds (**2** & **3)** were synthesized according to the slightly modified procedure already described in literature [28]. Briefly, in a typical reaction, sulfonyl chloride (10 mmol) as solution in THF (10 ml) was taken in round bottom flask. Hydrazine monohydrate (0.88 ml, 15 mmol) was added dropwise to reaction mixture maintaining the temperature at 10–15 ^{o}C followed by further stirring for 30 minutes at the same temperature. Ice cold water was added to the reaction mixture for precipitation of respective compounds **2 & 3** as colorless solids.

Compound **2** was obtained as colorless solid; R_f (EtOAc:Hexane 1:1); 0.35 and yield 82%. Compound **3** was obtained as colorless solid; R_f (EtOAc:Hexane 1:1); 0.22 and yield 71%.

(Z)-N'-(1-Allyl-2-oxoindolin-3-ylidene)methanesulfono-hydrazide (**4**)

Methanesulfonylhydrazide **2** (0.13 g, 1.2 mmol, 1.2 equiv.) and *N*-allylisatin **1** (0.187 g, 1.0 mmol) were refluxed for 3 hours in ethanol (10 ml) containing five drops of acetic acid according to the literature procedure [28] (for general procedure see supplementary material). Title compound **4** was obtained as yellow powder (0.223 g, 80%); R_f (EtOAc/Hexane, 1:4) 0.21; M.P. 162–165 ^{o}C;

UV/Vis. (λ_{max}, 0.1 mmol, acetonitrile) 338 nm; FT-IR (neat, cm^{-1}) 3169 (N-H, Str), 3006 (C-H, Ar), 2926 (C-H, Alkane), 1690 (C=O, Str), 1616 (C=N, Str), 1468 (C-C, Ar), 1341, 1166 (S=O, Str), 748 (C-H, (Bend) Ar). ^{1}H NMR (400 MHz, $CDCl_3$) δ 12.53 (s, 1H, NH), 7.87 (d, 1H, J = 7.8 Hz), 7.63 (t, 1H, J = 7.5 Hz), 7.30 (t, 1H, J = 7.8 Hz), 7.17 (d, 1H, J = 7.5 Hz), 5.83 (ddt, 1H, J = 16.0 Hz, 10.5 Hz, 5.2 Hz), 5.34 – 5.19 (m, 2H), 4.37 (d, 2H, J = 5.2 Hz), 2.83 (s, 3H, CH_3).^{13}C NMR (100 MHz, $CDCl_3$) δ 160.1 (C=O), 141.9 (C), 133.1 (C), 131.3 (CH), 130.7 (CH), 129.6 (CH), 121.5 (CH), 119.3 (=CH_2), 118.2 (C), 109.8 (CH), 43.1 (N-CH_2), 40.3 (CH_3).

(Z)-N'-(1-Allyl-2-oxoindolin-3-ylidene)-3-nitrobenzenesulfono-hydrazide **(5)**

3-Nitrobezenesulfonylhydrazide (0.26 g, 1.2 mmol, 1.2 equiv.) and *N*-allylisatin **1** (0.187 g, 1.0 mmol) were refluxed for 3 hours in ethanol (10 ml) containing five drops of acetic acid according to the reported procedure [28] (for general procedure see supplementary material). Title compound **5** was obtained as orange powder (0.320 g, 83%); M.P. 178 –180 ^{o}C; R_f (EtOAc/Hexane, 3:7), 0.40; UV/Vis. (λ_{max}, 0.1 mmol, acetonitrile), 353 nm; FT-IR (neat, cm^{-1}) 3109 (N-H, Str), 3033 (C-H, Ar), 2922 (C-H, Alk), 1685 (NC=O, Str), 1616 (C=N, Str), 1533 (N-O, Str), 1470 (C-C, Ar), 1355, 1175 (S=O, Str), 762 (C-H, (Bend) Ar); ^{1}H NMR (400 MHz, $CDCl_3$) δ 12.57(s, 1H, NH), 8.03(br.d, 2H, J = 7.3), 7.65–7.58 (m, 2H), 7.57– 7.50(m, 1H), 7.33(t, 1H, J = 7.8), 7.10(t, 1H, J = 7.6), 6.85(d, 1H, J = 7.8), 5.81(ddt, 1H, J = 15.9 Hz, 10.5 Hz, 5.3 Hz), 5.31–5.17(m, 2H), 4.34(d, 2H, J = 5.3 Hz); ^{13}C NMR (100 MHz, $CDCl_3$) δ 160.9 (C=O), 148.5 (C), 142.7 (C), 138.7(C), 135.5 (C), 133.6 (C), 133.1 (CH), 131.4 (CH), 130.6 (CH), 129.3 (CH), 128.0 (CH), 123.5 (CH), 121.4 (CH), 119.5 (=CH_2), 118.5 (CH), 110.0 (CH), 42.1 (N-CH_2).

2.3 Crystallography

Single crystal X-ray diffraction studies are executed on Agilent Super Nova (Dual source) Agilent Technologies Diffractometer having microfocus Cu/Mo Kα radiation source. The final data collection is made with the help of CrysAlisPro software [29]. SHELXL–97 method in-built with X-Seed is used for final structure solution [30,31]. The all atoms other than hydrogen are refined anisotropically by using full–matrix least squares methods [32]. The final structures of both compounds **4** and **5** are accomplished through PLATON and ORTEP in built with WinGX [33,34]. H atoms of benzene rings and terminal methylene are positioned geometrically and treated as riding atoms with C–H = 0.93 Å and Uiso(H) = 1.2 Ueq(C) for carbons. The N-H hydrogen atoms are located through fourier map and refined with N-H = 0.80(2) - 0.86(2)Å with Uiso (*H*) = 1.2 Ueq for *N* atom. The methyl and methylene hydrogen atoms are also positioned geometrically and treated as riding atoms with [C–H = 0.96 Å, Uiso(H) = 1.5 Ueq(C)] and [C–H = 0.97 Å, Uiso(H) = 1.2 Ueq(C)] for methyl and methylene carbon atoms, respectively. The crystal data has been deposited at the Cambridge Crystallographic data center and the assigned CCDC numbers are 1579181 and 1579182 for **4** and **5**, respectively. Crystal data can be received free of charge on application to CCDC 12 Union Road, Cambridge CB21 EZ, UK. (Fax: (+44) 1223 336-033; e-mail: data_request@ccdc.cam. ac.uk.

2.4 DFT calculations

Computational simulations are performed by using GAUSSIAN 09 package [35], and geometries are analyzed the help of GaussView 5.0 [36]. The geometry optimization of both derivatives (**4**

and **5**) is performed by using DFT/B3LYP/6-31G (d,p) method. The X-ray crystal structures are used as reference for the computational studies. Vibrational analysis is performed at the same level of theory in order to confirm true optimization (all real vibrations are observed). FMOs and MEP analyses are executed at the same level of theory.

2.5 Molecular Docking methods

Molecular Operating Environment (MOE 2016:0802) software package is used for the docking simulations. Three-dimensional (3-D) structure of urease from Bacillus pasteurii is obtained from Protein Data Bank (PDB accession code 4UBP). Acetohydroxamic acid (HAE) is the native ligand. Molecular builder option of MOE is used to draw the structures of the molecules. The drawn molecules are energy minimized using MMFF94 forcefield. The native ligand HAE is re-docked in the binding site of the enzyme (4UBP) and root mean square deviation (RMSD) is computed. The computed rmsd value is 0.89 Å. This confirms the reliability of our docking program.

Finally, the prepared compounds are docked into the binding site of the enzyme using Triangular Matching docking method. For each compound, 10 different conformations are allowed to be generated. In order to obtain minimum energy, the ligands are allowed to be flexible. The remaining parameters are maintained at their default settings. The best conformation of each compound–enzyme complex is ranked by GBVI/WAS binding free energy calculation. The lowest energy ligand-enzyme complex for each compound is selected and the resulting ligand-enzyme complexes are used for two-dimensional (2-D) and three-dimensional (3-D) interaction studies. 2-D docking results are viewed by using ligand interaction module implemented MOE. While, 3-D interaction plots are generated by using Discovery Studio Visualizer [37].

2.6 Urease Inhibition Assay

Urease inhibition of the synthesized compounds is assayed using modified Berthelot method [38]. The experimental details are exactly same as we have reported in our previous paper [28]. The % age inhibition is calculated with the help of mathematical expression given below:

$$\text{Inhibition (\%)} = 100 - \left(\frac{\text{Abs. of test sample}}{\text{Abs. of control}} \right) \times 100$$

IC_{50} values (conc. of inhibitor responsible for 50% inhibition of the enzymatic activity) of both compounds are calculated by measuring activities at further dilutions after computing the data by using EZ-Fit Enzyme software (Perrella Inc, USA) (units of absorbance of un-inhibited enzyme are between 1.0 and 1.2).

3 Results and discussion

Synthesis of the both compounds **4** and **5** is accomplished according to the scheme, given in the Fig. 1. First of all *N*-alkylation of the isatin is accomplished through nucleophilic substitution using allyl bromide under basic conditions in DMF to afford *N*-allylisatin as intermediate **1** in high yield. In parallel, two different sulfonyl chlorides are treated with hydrazine monohydrate in THF to form respective sulfonylhydrazides **2** and **3** in good yields. Synthesis of final compounds **4** and **5** is carried out by condensing the *N*-allylisatin derivative **1** with sulfonyhydazides **2** and **3** separately, in boiling ethanol and catalytic acetic acid (5 drops).

3.1 Single crystal X-ray diffraction analysis

Single crystal X-ray diffraction analysis is not only helpful us to confirm and decide about the final structures of compounds, but also provides the information about inter and intramolecular interactions among the molecules in the unit cell which are vital to stability of the compounds [39]. The single crystal X-ray parameters along with other structural information's of both **4** and **5** are given in the Table 1. The *ORTEP* plots of both hydrazides are shown in the Fig. 2.

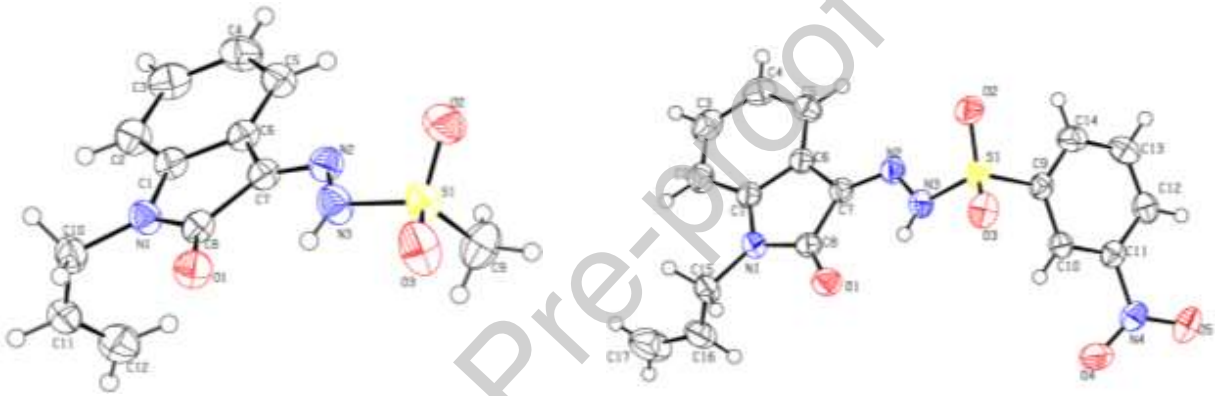

4 **5**

Fig. 2: The *ORTEP* plots of compounds **4** and **5**, thermal ellipsoids were drawn at 50% probability level

Both hydrazides (**4** and **5**) adopted the monoclinic crystal system and structures are solved with P 21/c and P21/n space groups, respectively. One independent molecule was observed in each case. It is well established from previously reported crystallographic studies that < O-S-O value is observed about 120º in sulfonamide containing molecules [40,41], and in the present both molecules the almost similar values are observed *i.e.* O3-S1-O2 angles are 119.56 (1)º and 121.51(9)º in **4** and **5**, respectively. This ultimately produced the distorted tetrahedral geometry

around *S* atom.

The root mean square (r.m.s.) deviation for the fitted atoms of indole ring (C1-C8/N1) in the both **4** and **5** are 0.0116(1) Å and 0.0112(1) Å, which suggest the planarity of the indole moiety. This was further verified with the help of dihedral angles between the fused benzene (C1-C6) and pyrrole (C1/C6/C7/C8/N1) rings which are 1.564(1)º and 1.471(1)º for molecule **4** and **5** respectively. Propylene (C10/C11/C12 for molecule **4** and C15/C16/C17 for molecule **5**) side chain which is attached to the nitrogen atom is oriented at dihedral angles of 77.25(2)º and 77.33(2)º with respect to the pyrrole (C1/C6/C7/C8/N1) rings in molecules **4** and **5**, respectively. In the molecule **5**, the nitrophenyl ring (C9-C14) is oriented at dihedral angle of 61.37(5)º with respect to indole functionality (C1-C8/N1). The nitro group N4/O4/O5 is twisted at dihedral angle of 23.94(2)° with respect to its parent aromatic ring (C9-C14). Unit cell diagrams (Fig. 3) of both compounds **(4** and **5)** show number of intra and inter non-covalent interactions. The oxygen atom of carbonyl (O1) of pyrrole linked to the hydrogen of hydrazide to form N3-H3N…O1 type intramolecular interaction and generate six membered ring motif *S*(6) in both compounds [42]. For these interactions <D-H-A angles are 131.1(2)° and 136.9(2)°, respectively whereas D-A distances are 2.77(2)Å and 2.73(2)Å while H-A distances are 2.19(2)Å and 2.06(2)Å for compound **4** and **5**, respectively. Due to presence of C-H…O type week interactions (atom numbering and other values are provided in Table 2) the inversion dimers are formed and further produce ten membered ring motif in molecule **5** while eighteen membered ring motif in molecule **4**. These dimers further connected through another C-H…O interactions to produce long zig-zag chains along *c*-axis in both compounds (Table 2).

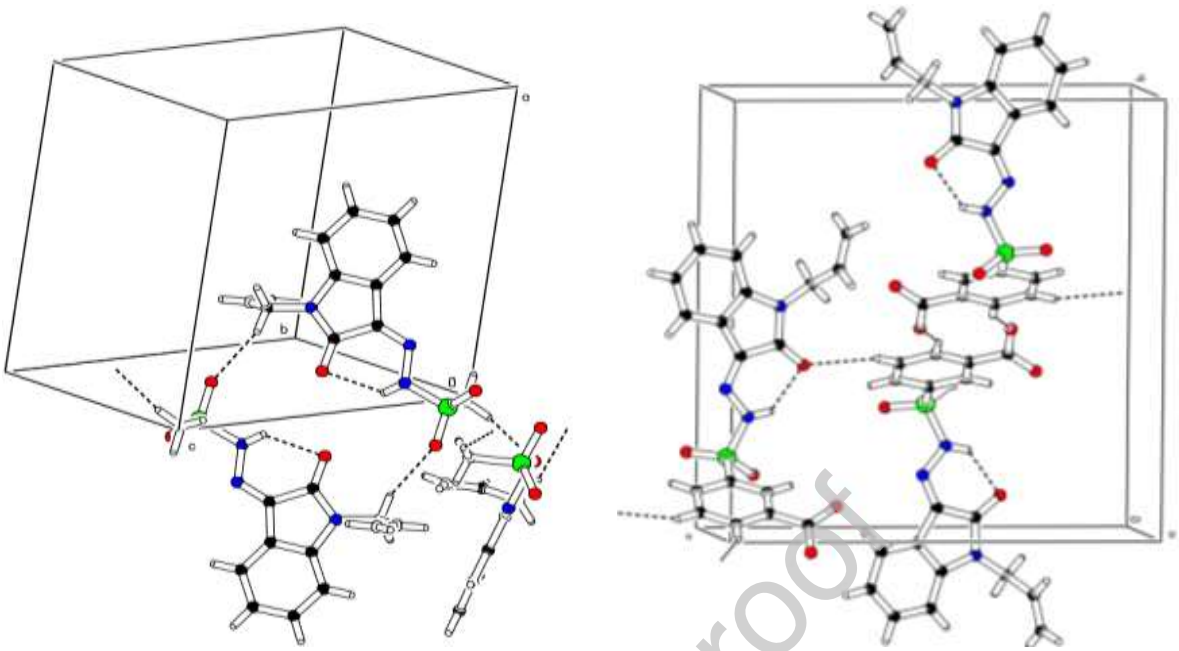

4 **5**

Fig. 3: Unit cell view of **4** and **5** showing non-covalent interactions

3.2 Molecular geometries

Experimental X-ray geometries provide basic guidelines for validating the theoretical method through comparison of geometric parameters. Therefore, we have optimized the geometries of compounds **4** and **5** at B3LYP/6-31G (d, p) method and compared with the geometric parameters obtained from experiment [43,44]. The energy minima structures of both hydrazides **4** and **5** are shown in the Fig. 4. Simulated and experimental bond lengths and bond angles of both derivatives **4** and **5** are given in Table 3 and Table 4, respectively.

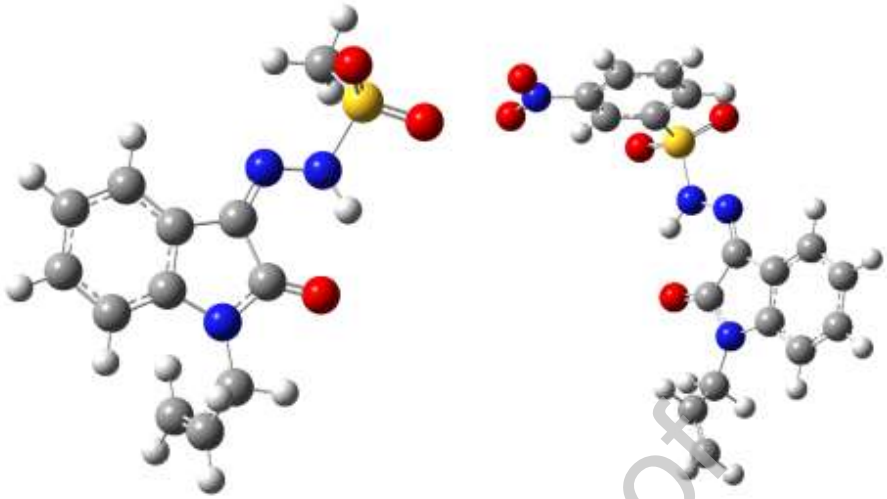

4 **5**

Fig. 4: Energy minima geometries of compounds **4** and **5**

X-ray diffraction values of vital bonds such as S1-N3, S1-O2, S1-O3, S1-C9, O1-C8, N2-N3, N2-C7, C8-N1, N1-C1 and N1-C10 (atomic labels are according to the *ORTEP* plot shown in Fig. 2) in (**4**) are 1.65Å, 1.41Å, 1.41Å, 1.74Å, 1.21Å, 1.36Å, 1.28Å, 1.36Å, 1.40Å and 1.44Å, respectively. The quantum chemical values of same bonds are 1.71Å, 1.45Å, 1.46Å, 1.79Å, 1.23Å, 1.34Å, 1.29Å, 1.38Å, 1.41Å and 1.45Å, respectively and corroborated nicely with the experimental results. The X-ray diffraction values of bonds C1-N1, C7-N2, C8-N1, C8-O1, C9-S1, C11-N4, C15-N1, N4-O4, N4-O5, N2-N3, N3-S1, O2-S1 and O3-S1 bonds in **5** are 1.41Å, 1.28Å, 1.36Å, 1.22Å, 1.76Å, 1.46Å, 1.46Å, 1.22Å, 1.22Å, 1.35Å, 1.63Å, 1.42Å and 1.41Å, respectively. Quantum chemical analysis of same bonds showed nice correlation with experiment and are observed at 1.41Å, 1.29Å, 1.37Å, 1.23Å, 1.79Å, 1.47Å, 1.45Å, 1.22Å, 1.22Å, 1.33Å, 1.69Å, 1.45Å and 1.46Å, respectively.

The X-ray diffraction and quantum chemical results showed that vital bond angles of both sulfonamides **4** and **5** have very excellent correlation with each other. The experimental values of important bond angles of **4** such as N3-S1-C9, O2-S1-N3, O2-S1-C9, O3-S1-N3, O3-S1-O2, O3-S1-C9, C7-N2-N3, N2-N3-S1, O1-C8-N1, O1-C8-C7, N1-C8-C7, C8-N1-C1, C8-N1-C10, C1-N1-C10, C6-C1-N1, C2-C1-N1, N1-C10-C11, N2-C7-C8, and N2-C7-C6 (atomic labels are with reference to Fig. 2) are 105.1^{o}, 107.5^{o}, 108.8^{o}, 104.9^{o}, 119.5^{o}, 109.7^{o}, 118.0^{o}, 114.4^{o}, 126.8^{o}, 106.2^{o}, 110.7^{o}, 124.8^{o}, 124.8^{o}, 110.1^{o}, 127.8^{o}, 113.7^{o}, 127.7^{o}, and 125.9^{o} respectively. The theoretical values of respective bond angles are 100.9^{o}, 110.5^{o}, 107.9^{o}, 102.9^{o}, 121.8^{o}, 110.4^{o}, 118.2^{o}, 117.5^{o}, 126.3^{o}, 127.2^{o}, 106.3^{o}, 110.4^{o}, 123.0^{o}, 126.3^{o}, 107.9^{o}, 128.6^{o}, 115.2^{o}, 126.3^{o}, and 126.8^{o} respectively. Again, the X-ray diffraction and quantum chemical results of vital bond angles of hydrazide **5** reflect the excellent correlation with each other (for detailed values see Table 4).

3.3 Frontier molecular orbitals and UV-vis analyses

FMOs analysis of both derivatives is performed for understanding the reactivity and kinetic stability [45]. The FMOs surfaces of both compounds **4** and **5** are shown in the Fig. 5.

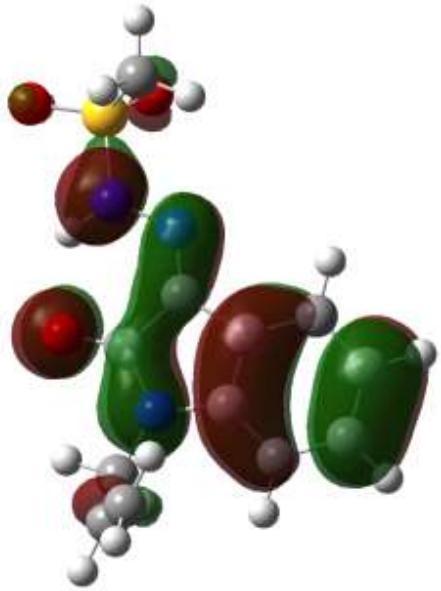

HOMO (4)

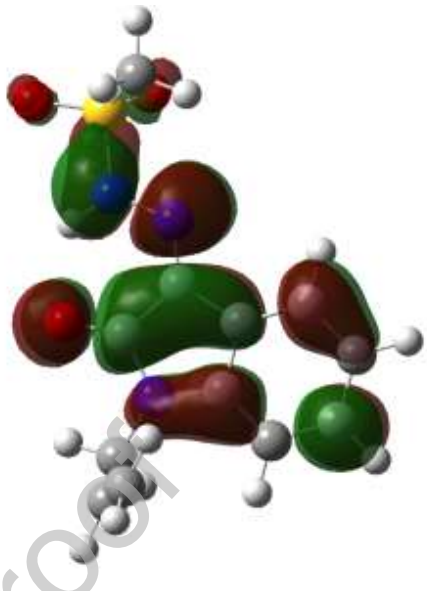

LUMO (4)

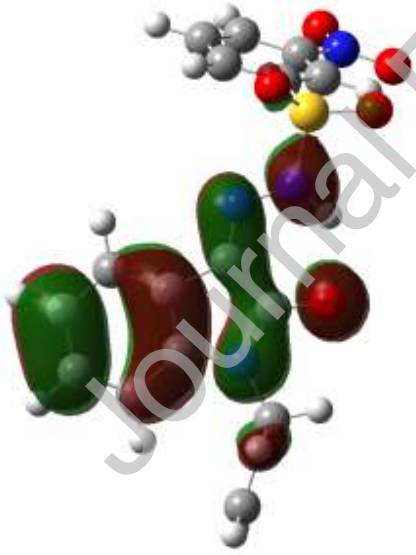

HOMO (5)

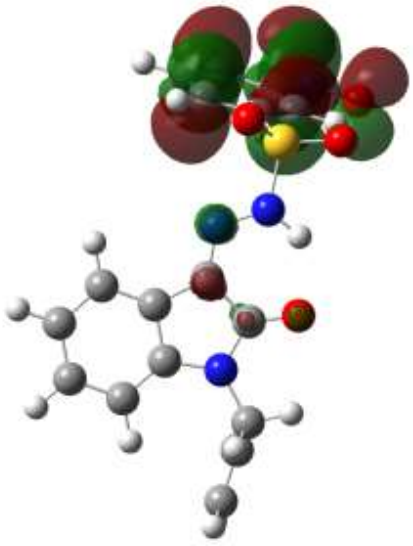

LUMO (5)

Fig. 5 FMOs surfaces of both compounds **4** and **5**

It is cleared from the HOMO/LUMO surfaces of both compounds, that dispersion of isodensity is different in both. In one the π-electronic cloud is mainly dispersed on isatin moiety, which reflects

that the electronic transitions occurs in isatin and enone functionality attached to it. In **5**, the dispersion of isodensity is totally different. The π-electronic cloud in HOMO is dispersed mainly on isatin, whereas the in LUMO is shifted toward the nitro benzene ring, which is may be due to the electron withdrawing nature of nitro group. In **5**, the electronic transitions occur between isatin and nitrobenzene moieties. The HOMO and LUMO energies of compound **4** are -6.12 eV and -2.26 eV, respectively. The H-L_G of compound **4** is 3.86 eV. The HOMO, LUMO energies and respective H-L_G of compound **5** are -6.22 eV, -2.81 eV and 3.41 eV, respectively. The absorption analysis is performed by using TD-DFT level of theory at B3LYP/6-31G(d,p) method. Based on DFT calculations the energy gap of **4** is 4.03 eV and corresponding λ_{max} is 307 nm. For compound **5** the energy gap is 3.94 eV along the corresponding λ_{max} is 314 nm. The energy gap values reflect that **4** is more stable than the compound **5**. The absorption analysis revealed that in **4** the major excitation occurs from HOMO-1 to LUMO, whereas in **5** it occurs from HOMO-1 to LUMO+1 orbital.

3.4 Molecular electrostatic potential (MEP) analysis

MEP analysis is a global property and gives the idea about the electronic distribution in a compound [46]. The MEP surfaces of both compounds are extracted from the energy minima structures and shown in Fig. 6. The MEP analysis shows that both compounds are nucleophilic in nature and have strong affinity for positively charged species. The electronegative potential on compound **4** is localized on the sulfonamide and C=O moieties, whereas in **5** it is also located on nitro group along with the previous moieties. The dispersion of electronic density of **4** is in the range of -0.051 to 0.051 esu, whereas in **5** it is dispersed in the range of -0.045 to 0.045 esu.

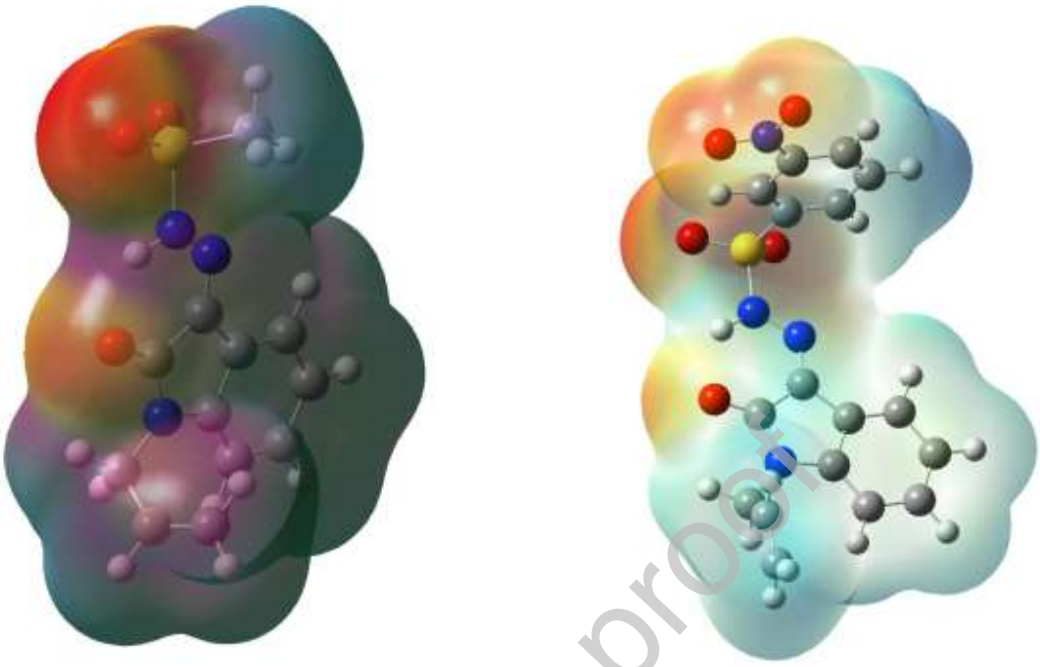

Fig. 6 MEP surfaces of both compounds **4** and **5**

3.5 Urease inhibition assay

In vitro enzyme inhibition bioassay of both **4** and **5** is performed against urease enzyme and results are mentioned in Table 5. Both showed good to excellent urease inhibition efficiency, determined at 0.5 mM concentration. Both compounds showed IC_{50} values in uM concentration range. As mentioned in Table 5, compound **4** exhibited better efficacy against the enzyme with least IC_{50} value of 15.26 ± 0.16 µM compared to the standard thiourea showing 21.25±0.15 µM. On the other hand, compound **5** showed higher IC_{50} value (58.78±0.12 µM). % Inhibition of both compounds is also measured at 0.5 mM concentration. The compound **4** has 92.75±0.22 % inhibition, whereas **5** has 75.44±0.23 % inhibition as compared to the standard (98.45±0.87).

3.6 Molecular docking investigations

The binding orientation of all the synthesized isatin derivatives in the binding site of *Bacillus pasteurii* was explored using docking simulations. Crystal structure of *B. pasteurii* urease with acetohydroxamic acid (HAE) as a native ligand was obtained from Protein Data Bank (PDB code 4UBP) [47]. Docking simulations were carried out by using Molecular Operating Environment (MOE 2016.08) [48]. The native ligand HAE was re-docked in the binding site of the enzyme (4UBP) and root mean square deviation (RMSD) is computed. The computed rmsd value is 0.89 Å. This confirms the reliability of our docking program.

The visual inspection of the best-scored highly active isatin derivative **4** (IC_{50}=15.26 ± 0.16 µM) revealed that it coordinates with Ni798 and Ni799 *via* sulfonyl oxygen atoms. His275 is involved in hydrogen bond interactions with one of the sulfonyl oxygen. While, His222 establishes hydrogen bond interaction (HBI) with another sulfonyl oxygen and isatin oxygen. Another important HBI was found between Asp363 and –NH of sulfonyl hydrazide (Fig. 7).

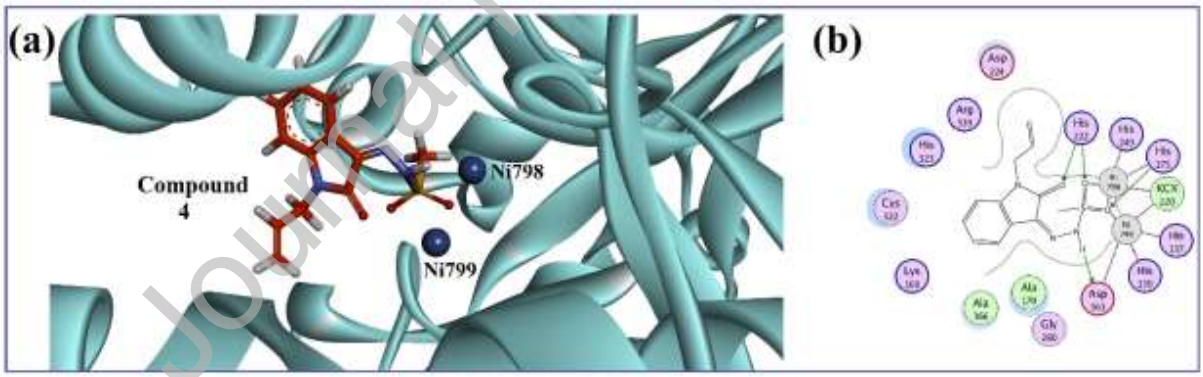

Fig. 7 (a) Three-dimensional modelled diagram of compound 4 into the binding site of 4UBP. Nickel ions are shown in blue spheres. (**b**) Two-dimensional **(**2D) interactions plot of compound **4** into the binding site of 4UBP.

In vitro activity data presented in Table 5 showed that moving from methanesulfonohydrazide **4** to 3-nitrobenzenesulfonohydrazide **5** (IC_{50}=58.78 ± 0.12 µM) the activity decreases almost 4 times. The binding orientation of compound **5** superimposed on native ligand HAE is shown in Fig. 8. It

can be seen that **5** binds away from the nickel bi-center and forms π-alkyl type of interaction with Ala170 (Fig. 8**)**. Isatin carbonyl group and –NH of sulfonyl hydrazide forms HBI with Cys322. Nitro group forms HBI with Hus323 and Arg339.

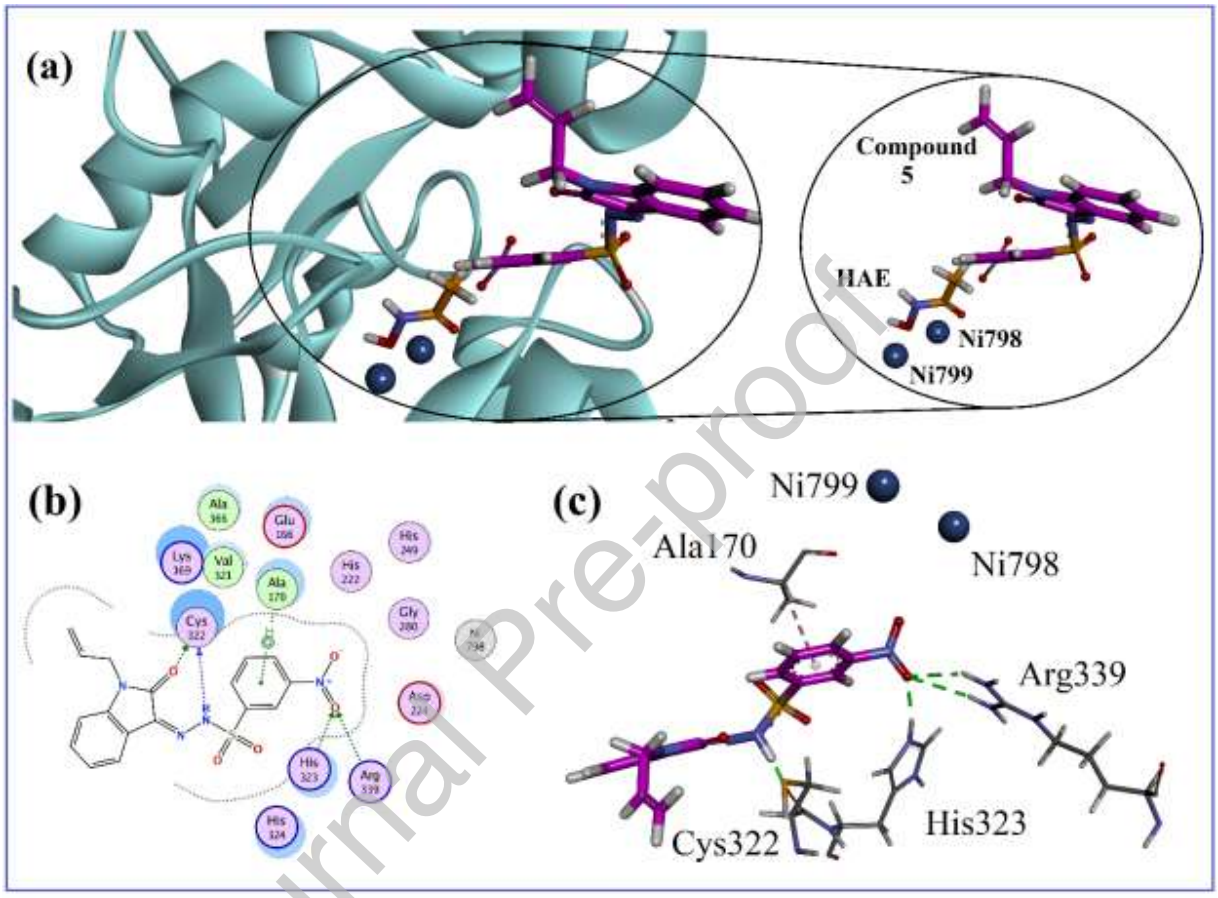

Fig. 8 (a) Depiction of the lowest energy docking-poses of the compound **5** (pink) superimposed on the native ligand HAE (yellow) into the binding site of *B. pasteurii* urease (PDB ID 4UBP). A ribbon model of the enzyme is presented; **(b)** 2D interactions of **5; (c)** 3-D interaction plot generated by Discovery Studio Visualizer (hydrogen bond interactions are shown as green dotted line)

The docking results of the compounds **4** and **5** revealed that compound **4** binds deep into the binding site of the 4UBP interacting with Ni^{2+} ions. However, our docking simulation results showed that due to bulky nitro group, compound **5** is located 4.16 Å and 5.45 Å away from Ni798 and Ni799 respectively (Figure 9). It binds to the active site flap (gate-residues) residues. Apart

from the active site architecture of *B. Pasteurii* urase (BPU) containing two Ni ions and histidine residues, residues at the flap of the active site also involves in its activation. Among them, Cys322 is an important flap residue and is involved in the positioning of other active site residues. Other residues of flap region are: Arg339 and Ala170. It can be concluded here that compound 5 restrict the mobility of the active site flap by interacting with Cys322.

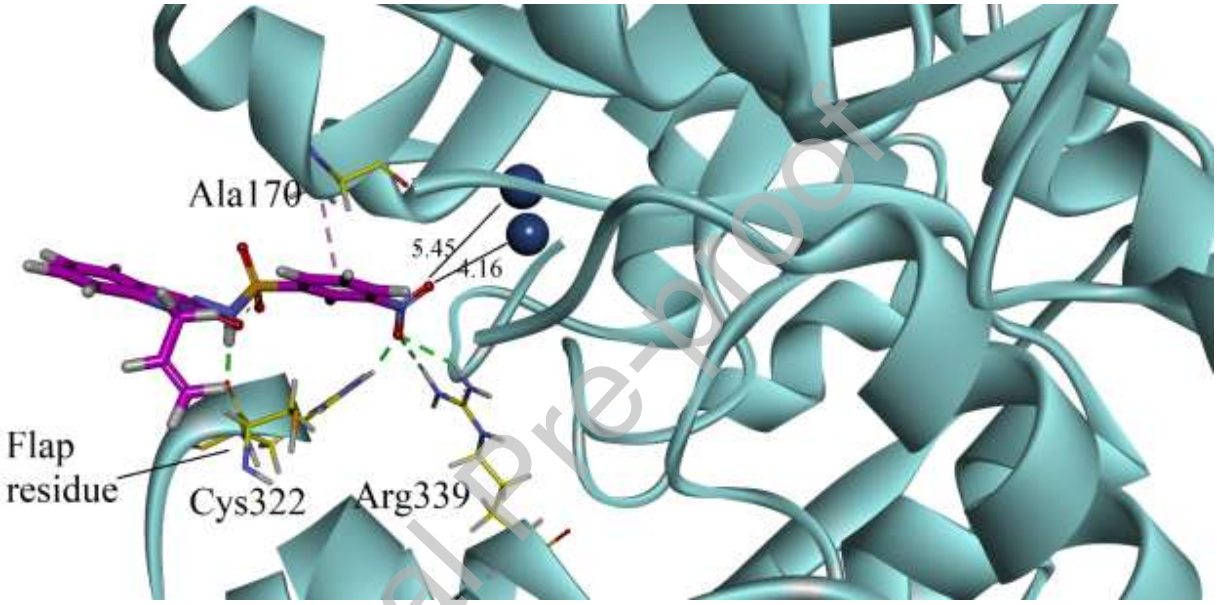

Fig. 9: 3-D modelled ribbon diagram of compound **5** into the binding site of *B. pasteurii* urease (PDB ID 4UBP) showing the distance between two Ni ions and oxygen atom of nitro group (black solid lines). The interaction with flap residues is also shown (dotted lines).

4 Conclusions

We have successfully accomplished the synthesis of two new sulfono-hydrazides **4** and **5** from *N*-allylisatin and their structures are fully characterized with the help of different kind of spectroscopic techniques. Both compounds have suitable crystals, which are subjected to the single crystal X-ray diffraction analysis. The single crystal X-ray data of both **4** and **5** is compared with the DFT calculations. The quantum chemical data is proved in full agreement with the X-ray

diffraction values. Both compounds showed urease inhibition activity *in vitro* with **4** showing better results and thus making it more attractive motif for further studies in drug discovery and development. Docking simulations revealed that highly active compound **4** coordinates deeply with Ni798 and Ni799 of of *Bacillus pasteurii*.

Acknowledgements

The project was funded by the Deanship of Scientific Research (DSR), King Abdulaziz University, Jaddah, Saudi Arabia under grant no; (DF-614-130-1441). The authors, therefore, gratefully acknowledge the DSR technical and financial support.

Authors declaration

We the undersigned declare that this manuscript is original, has not been published before and is not currently being considered for publication elsewhere.

We wish to confirm that there are no known conflicts of interest associated with this publication and there has been no significant financial support for this work that could have influenced its outcome.

We confirm that the manuscript has been read and approved by all named authors and that there are no other persons who satisfied the criteria for authorship but are not listed. We further confirm that the order of authors listed in the manuscript has been approved by all of us.

We confirm that we have given due consideration to the protection of intellectual property associated with this work and that there are no impediments to publication, including the timing of publication, with respect to intellectual property. In so doing we confirm that we have followed the regulations of our institutions concerning intellectual property.

We understand that the Corresponding Author is the sole contact for the Editorial process (including Editorial Manager and direct communications with the office). He is responsible for communicating with the other authors about progress, submissions of revisions and final approval of proofs. We confirm that we have provided a current, correct email address which is accessible by the Corresponding Author.

Credit author statement

All persons who meet authorship criteria are listed as authors, and all authors certify that they have participated sufficiently in the work to take public responsibility for the content, including participation in the concept, design, analysis, writing, or revision of the manuscript. Furthermore, each author certifies that this material or similar material has not been and will not be submitted to or published in any other publication before its appearance in the *Optics and Laser Technology*

Authorship contributions

Muhammad Arshad, **Kainat Ahmed** and **Zafar Iqbal**: Synthesis, Enzyme inhibition, Writing-Original draft preparation. Visualization, Investigation

Umer Rashid: Molecular docking, Software

Muhammad Nadeem Arshad, Abdullah M. Asiri: X-ray analysis, Writing- Reviewing and Editing

Tariq Mahmood: DFT, Writing- Reviewing and Editing, Supervision

References

[1] J.F.M. da Silva, S.J. Garden, A.C. Pinto, The chemistry of isatins: a review from 1975 to 1999, J. Braz. Chem. Soc. 12 (2001) 273–324.

[2] P. Pakravan, S. Kashanian, M.M. Khodaei, F.J. Harding, Biochemical and pharmacological characterization of isatin and its derivatives: from structure to activity, Pharmacol. Reports. 65 (2013) 313–335.

[3] M.-G.A. Shvekhgeimer, Synthesis of heterocyclic compounds by the cyclization of isatin and its derivatives (review), Chem. Heterocycl. Compd. 32 (1996) 249–276.

[4] A. Farag, Synthesis and Antimicrobial Activity of 5-(morpholinosulfonyl)isatin Derivatives Incorporating a Thiazole Moiety, Drug Res. (Stuttg). 65 (2014) 373–379.

[5] Y.-O. Teng, H.-Y. Zhao, J. Wang, H. Liu, M.-L. Gao, Y. Zhou, K.-L. Han, Z.-C. Fan, Y.-M. Zhang, H. Sun, P. Yu, Synthesis and anti-cancer activity evaluation of 5-(2-carboxyethenyl)-isatin derivatives, Eur. J. Med. Chem. 112 (2016) 145–156.

[6] D. Jiang, G.-Q. Wang, X. Liu, Z. Zhang, L.-S. Feng, M.-L. Liu, Isatin Derivatives with Potential Antitubercular Activities, J. Heterocycl. Chem. 55 (2018) 1263–1279.

[7] V. Jupally, V. Eggadi, S.B. Sheshagiri, U. Kulandaivelu, Synthesis and evaluation of neuropharmacological profile of isatin-3-[N 2 -(2-benzalaminothiazol-4-yl)] hydrazones,

Egypt. Pharm. J. 14 (2015) 130.

[8] K. L. Vine, L. Matesic, J. M. Locke, D. Skropeta, eds., Recent Highlights in the Development of Isatin-Based Anticancer Agents, in: Adv. Anticancer Agents Med. Chem., BENTHAM SCIENCE PUBLISHERS, 2013: pp. 254–312.

[9] C. Le Tourneau, E. Raymond, S. Faivre, Sunitinib: a novel tyrosine kinase inhibitor. A brief review of its therapeutic potential in the treatment of renal carcinoma and gastrointestinal stromal tumors (GIST), Ther. Clin. Risk Manag. 3 (2007) 341–348.

[10] L. Richeldi, R.M. du Bois, G. Raghu, A. Azuma, K.K. Brown, U. Costabel, V. Cottin, K.R. Flaherty, D.M. Hansell, Y. Inoue, D.S. Kim, M. Kolb, A.G. Nicholson, P.W. Noble, M. Selman, H. Taniguchi, M. Brun, F. Le Maulf, M. Girard, S. Stowasser, R. Schlenker-Herceg, B. Disse, H.R. Collard, Efficacy and Safety of Nintedanib in Idiopathic Pulmonary Fibrosis, N. Engl. J. Med. 370 (2014) 2071–2082.

[11] O.D. Lopina, Enzyme Inhibitors and Activators, in: Enzym. Inhib. Act., InTech, 2017.

[12] U. Rashid, F. Rahim, M. Taha, M. Arshad, H. Ullah, T. Mahmood, M. Ali, Synthesis of 2-acylated and sulfonated 4-hydroxycoumarins: In vitro urease inhibition and molecular docking studies, Bioorg. Chem. 66 (2016) 111–116.

[13] W. Lankes, K. Fleischer, D.C. Gulba, Direkte Thrombinantagonisten, Herz. 26 (2001) S46–S52.

[14] S.T. Tanoli, M. Ramzan, A. Hassan, A. Sadiq, M.S. Jan, F.A. Khan, F. Ullah, H. Ahmad, M. Bibi, T. Mahmood, U. Rashid, Design, synthesis and bioevaluation of tricyclic fused

ring system as dual binding site acetylcholinesterase inhibitors, Bioorg. Chem. 83 (2019) 336–347.

[15] C.L. Deasy, The Mechanism of Urease Inhibition by Urea, J. Am. Chem. Soc. 69 (1947) 294–295.

[16] M. Hanif, K. Shoaib, M. Saleem, N. Hasan Rama, S. Zaib, J. Iqbal, Synthesis, Urease Inhibition, Antioxidant, Antibacterial, and Molecular Docking Studies of 1,3,4-Oxadiazole Derivatives, ISRN Pharmacol. 2012 (2012) 1–9.

[17] H. Carlsson, E. Nordlander, Computational Modeling of the Mechanism of Urease, Bioinorg. Chem. Appl. 2010 (2010) 1–8.

[18] S. Svane, J.J. Sigurdarson, F. Finkenwirth, T. Eitinger, H. Karring, Inhibition of urease activity by different compounds provides insight into the modulation and association of bacterial nickel import and ureolysis, Sci. Rep. 10 (2020) 8503.

[19] A. Balasubramanian, K. Ponnuraj, Crystal Structure of the First Plant Urease from Jack Bean: 83 Years of Journey from Its First Crystal to Molecular Structure, J. Mol. Biol. 400 (2010) 274–283.

[20] E.M.F. Muri, H. Mishra, M.A. Avery, J.S. Williamson, Design and Synthesis of Heterocyclic Hydroxamic Acid Derivatives as Inhibitors of Helicobacter pylori Urease, Synth. Commun. 33 (2003) 1977–1995.

[21] Y.F. Rego, M.P. Queiroz, T.O. Brito, P.G. Carvalho, V.T. de Queiroz, Â. de Fátima, F. Macedo Jr., A review on the development of urease inhibitors as antimicrobial agents

against pathogenic bacteria, J. Adv. Res. 13 (2018) 69–100.

[22] K.M. Khan, S. Iqbal, M.A. Lodhi, G.M. Maharvi, Z.- Ullah, M.I. Choudhary, A.- Rahman, S. Perveen, Biscoumarin: new class of urease inhibitors; economical synthesis and activity, Bioorg. Med. Chem. 12 (2004) 1963–1968.

[23] K. Mohammed Khan, Z.S. Saify, M. Arif Lodhi, N. Butt, S. Perveen, G. Murtaza Maharvi, M. Iqbal Choudhary, Atta-ur-rahman, Piperidines: A new class of Urease inhibitors, Nat. Prod. Res. 20 (2006) 523–530.

[24] H. Pervez, Z.H. Chohan, M. Ramzan, F.-U.-H. Nasim, K.M. Khan, Synthesis and biological evaluation of some new N 4 -substituted isatin-3-thiosemicarbazones, J. Enzyme Inhib. Med. Chem. 24 (2009) 437–446.

[25] A.F. Butt, M.N. Ahmed, M.H. Bhatti, M.A. Choudhary, K. Ayub, M.N. Tahir, T. Mahmood, Synthesis, structural properties, DFT studies, antimicrobial activities and DNA binding interactions of two newly synthesized organotin(IV) carboxylates, J. Mol. Struct. 1191 (2019) 291–300.

[26] M. Madni, M.N. Ahmed, S. Hameed, S.W. Ali Shah, U. Rashid, K. Ayub, M.N. Tahir, T. Mahmood, Synthesis, quantum chemical, in vitro acetyl cholinesterase inhibition and molecular docking studies of four new coumarin based pyrazolylthiazole nuclei, J. Mol. Struct. 1168 (2018) 175–186.

[27] M.N. Ahmed, K.A. Yasin, S. Hameed, K. Ayub, I. Haq, M.N. Tahir, T. Mahmood, Synthesis, structural studies and biological activities of three new 2-(pentadecylthio)-5-aryl-1,3,4-oxadiazoles, J. Mol. Struct. 1129 (2017) 50–59.

[28] M. Arshad, M. Jadoon, Z. Iqbal, M. Fatima, M. Ali, K. Ayub, A.M. Qureshi, M. Ashraf, M.N. Arshad, A.M. Asiri, A. Waseem, T. Mahmood, Synthesis, molecular structure, quantum mechanical studies and urease inhibition assay of two new isatin derived sulfonylhydrazides, J. Mol. Struct. 1133 (2017) 80–89.

[29] Agilent CrysAlis PRO Agilent Technologies, Yarnton, England (2012).

[30] G.M. Sheldrick, Crystal structure refinement with SHELXL, Acta Crystallogr. Sect. C Struct. Chem. 71 (2015) 3–8.

[31] L.J. Barbour, X-Seed — A Software Tool for Supramolecular Crystallography, J. Supramol. Chem. 1 (2001) 189–191.

[32] G. D'Antona, The full least-squares method, IEEE Trans. Instrum. Meas. 52 (2003) 189–196.

[33] L.J. Farrugia, WinGX suite for small-molecule single-crystal crystallography, J. Appl. Crystallogr. 32 (1999) 837–838.

[34] L.J. Farrugia, WinGX and ORTEP for Windows : an update, J. Appl. Crystallogr. 45 (2012) 849–854.

[35] J.L., W.C. Frisch, M.J. Trucks, G.W. Schlegel, H.B. Scuseria, G.E. Robb, M.A. Cheeseman, J.R. Scalmani, G. Barone, V. Mennucci, B. Petersson, G.A. Nakatsuji, H. Caricato, M. Li, X. Hratchian, H.P. Izmaylov, A.F. Bloino, J. Zheng, G. Sonnenberg, Gaussian 09, Rev. C.01, Gaussian, Inc., Wallingford CT, 2010.

[36] R. Dennington, T. Keith, J. Millam, GaussView 5.0, Semichem Inc., 2009.

[37] Dassault Systèmes BIOVIA, Discovery Studio Modeling Environment, Release 4.5, San Diego:

Dassault Systèmes, 2015.

[38] M.W. Weatherburn, Phenol-hypochlorite reaction for determination of ammonia, Anal. Chem. 39 (1967) 971–974.

[39] M.N. Arshad, O. Şahin, M. Zia-ur-Rehman, I.U. Khan, A.M. Asiri, H.M. Rafique, 4-hydroxy-2H-1,2-benzothiazine-3-carbohydrazide 1,1-dioxide-oxalohydrazide (1:1): X-ray structure and DFT calculations, J. Struct. Chem. 54 (2013) 437–442.

[40] H.M. Faidallah, L.A. Taib, S.N.A. Albeladi, M.E.U. Rahman, F.A. Al-Zahrani, M.N. Arshad, A.M. Asiri, Synthesis, Crystal Structures and Cytotoxic Activity of New 1,3,4,5-tetrahydro-2H-1,5-benzodiazepine Derivatives, J. Chem. Res. 39 (2015) 502–508.

[41] M.N. Arshad, O. Şahin, M. Zia-ur-Rehman, M. Shafiq, I.U. Khan, A.M. Asiri, S.B. Khan, K.A. Alamry, Crystallographic Studies of Dehydration Phenomenon in Methyl 3-hydroxy-2-methyl-1,1,4-trioxo-1,2,3,4-tetrahydro-1λ 6-benzo[e][1,2]thiazine-3-carboxylate, J. Chem. Crystallogr. 43 (2013) 671–676.

[42] J. Bernstein, R.E. Davis, L. Shimoni, N.-L. Chang, Patterns in Hydrogen Bonding: Functionality and Graph Set Analysis in Crystals, Angew. Chemie Int. Ed. English. 34 (1995) 1555–1573.

[43] M.N. Arshad, A.M. Asiri, K.A. Alamry, T. Mahmood, M.A. Gilani, K. Ayub, A.S. Birinji, Synthesis, crystal structure, spectroscopic and density functional theory (DFT) study of N-[3-anthracen-9-yl-1-(4-bromo-phenyl)-allylidene]-N-benzenesulfonohydrazine, Spectrochim. Acta Part A Mol. Biomol. Spectrosc. 142 (2015) 364–374.

[44] N. Rasool, A. Kanwal, T. Rasheed, Q. Ain, T. Mahmood, K. Ayub, M. Zubair, K. Khan, M.

Arshad, A. M. Asiri, M. Zia-Ul-Haq, H. Jaafar, One Pot Selective Arylation of 2-Bromo-5-Chloro Thiophene; Molecular Structure Investigation via Density Functional Theory (DFT), X-ray Analysis, and Their Biological Activities, Int. J. Mol. Sci. 17 (2016) 912.

[45] S.S. Hamdani, B.A. Khan, M.N. Ahmed, S. Hameed, K. Akhter, K. Ayub, T. Mahmood, Synthesis, crystal structures, computational studies and α-amylase inhibition of three novel 1,3,4-oxadiazole derivatives, J. Mol. Struct. 1200 (2020) 127085.

[46] S. Sherzaman, Sadiq-ur-Rehman, M.N. Ahmed, B.A. Khan, T. Mahmood, K. Ayub, M.N. Tahir, Thiobiuret based Ni(II) and Co(III) complexes: Synthesis, molecular structures and DFT studies, J. Mol. Struct. 1148 (2017) 388–396.

[47] S. Benini, W.R. Rypniewski, K.S. Wilson, S. Miletti, S. Ciurli, S. Mangani, The complex of Bacillus pasteurii urease with acetohydroxamate anion from X-ray data at 1.55 Å resolution, JBIC J. Biol. Inorg. Chem. 5 (2000) 110–118.

[48] Molecular Operating Environment (MOE ver. 2016.0208), Chemical Computing Group Inc., 1010 Sherbrooke Street West, Suite 91, Montreal, H3A 2R7, Canada.

Tables 1-5

Table 1: Crystal data and structure refinement parameters of compounds **4** and **5**.

Compound	**4**	**5**
Empirical formula	$C_{12}H_{13}N_3O_3S$	$C_{17}H_{14}N_4O_5S$
Formula weight	279.31	386.38
Temperature/K	296(2)	296(2)
Crystal system	monoclinic	monoclinic
Space group	$P2_1/c$	$P2_1/n$
a/Å	11.3583(4)	7.2031(2)
b/Å	9.3092(4)	15.8805(6)
c/Å	12.1247(5)	14.8422(6)
α/°	90	90
β/°	95.850(4)	90.065(4)
γ/°	90	90
Volume/$Å^3$	1275.35(9)	1697.78(11)
Z	4	4
$\rho_{calc}mg/mm^3$	1.455	1.512
m/mm^{-1}	0.262	0.230
F(000)	584.0	800.0
Crystal size/mm^3	0.49 × 0.36 × 0.28	0.42 × 0.35 × 0.22
2Θ range for data collection	5.67 to 58.2°	5.49 to 58.412°
Index ranges	$-14 \le h \le 14$, $-11 \le k \le 10$, $14 \le l \le 16$	$-9 \le h \le 9$, $-20 \le k \le 20$, $19 \le l \le 20$
Reflections collected	6726	16433
Independent reflections	3062[R(int) = 0.0186]	4200[R(int) = 0.0324]
Data/restraints/parameters	3062/0/177	4200/0/247
Goodness-of-fit on F^2	1.035	1.035
Final R indexes [I>=2σ (I)]	R_1 = 0.0387, wR_2 = 0.0901	R_1 = 0.0434, wR_2 0.0970
Final R indexes [all data]	R_1 = 0.0529, wR_2 = 0.0997	R_1 = 0.0650, wR_2 0.1095
Largest diff. peak/hole / e Å	0.28/-0.35	0.20/-0.41

Table 2: Hydrogen Bonds information of both compounds **4** and **5**

Compound 4						
D	**H**	**A**	**d(D-H)/Å**	**d(H-A)/Å**	**d(D-A)/Å**	**D-H-A/°**
C1(	H10E	O3	0.97	2.37	3.276(2)	155.3
C9	H9B	O1	0.96	2.43	3.260(2)	144.2
N3	H3N	O1	0.80(2)	2.19(2)	2.776(2)	131.1(19)
[1]2-X,1-Y,-Z; [2]2-X,-1/2+Y,1/2-Z						
Compound 5						
D	**H**	**A**	**d(D-H)/Å**	**d(H-A)/Å**	**d(D-A)/Å**	**D-H-A/°**
C1	H12	O5	0.93	2.43	3.298(2)	155.2
C1	H13	O1	0.93	2.52	3.325(2)	144.5
N3	H3N	O1	0.84(2)	2.06(2)	2.732(2)	136.9(19)
[1]2-X,-Y,-Z; [2]1/2+X,1/2-Y,1/2+Z						

Table 3: Comparison of some important X-ray and simulated bond lengths (Å) of compounds **4** and **5** (Atomic labels are with reference *ORTEP* plots Fig. 2).

4	**X-ray**	**Calc.**	**5**	**X-ray**	**Calc.**
S1-N3	1.65 (16)	1.71	C1-N1	1.41 (2)	1.41
S1-O2	1.41 (14)	1.45	C7-N2	1.28 (2)	1.29
S1-O3	1.41 (13)	1.46	C8-N1	1.36 (2)	1.37
S1-C9	1.74 (2)	1.79	C8-O1	1.22 (2)	1.23
O1-C8	1.21 (19)	1.23	C9-S1	1.76 (18)	1.79
N2-N3	1.36 (2)	1.34	C11-N4	1.46 (2)	1.47
N2-C7	1.28 (2)	1.29	C15-N1	1.46 (2)	1.45
C8-N1	1.36 (2)	1.38	N4-O4	1.22 (2)	1.22
N1-C1	1.40 (19)	1.41	N4-O5	1.22 (19)	1.22
N1-C10	1.44 (2)	1.45	N2-N3	1.35 (2)	1.33
			N3-S1	1.63 (16)	1.69
			O2-S1	1.42 (14)	1.45
			O3-S1	1.41 (14)	1.46

Table 4: Comparison of some important X-ray and simulated bond angles (Å) of compounds **4** and **5** (Atomic labels are with reference *ORTEP* plots Fig. 2).

4	X-ray	Calc.	5	X-ray	Calc.
N3-S1-C9	105.1 (9)	100.9	C2-C1-N1	129.0 (16)	128.7
O2-S1-N3	107.5 (9)	110.5	C6-C1-N1	109.5 (15)	109.7
O2-S1-C9	108.8 (11)	107.9	C10-C11-N4	117.9 (15)	118.6
O3-S1-N3	104.9 (8)	102.9	C12-C11-N4	119.3 (16)	118.8
O3-S1-O2	119.5 (10)	121.8	N1-C15-C16	112.8 (16)	113.3
O3-S1-C9	109.7 (10)	110.4	O4-N4-C11	117.4 (15)	117.5
C7-N2-N3	118.0 (14)	118.2	O5-N4-C11	118.5 (16)	117.4
N2-N3-S1	114.4 (2)	117.5	O5-N4-O4	123.9 (16)	125.0
O1-C8-N1	126.8 (15)	126.3	C1-N1-C15	125.5 (15)	126.6
O1-C8-C7	126.8 (15)	127.2	N2-C7-C6	125.6 (15)	127.0
N1-C8-C7	106.2 (13)	106.3	N2-C7-C8	127.6 (16)	126.1
C8-N1-C1	110.7 (13)	110.4	N1-C8-C7	106.4 (14)	106.4
C8-N1-C10	124.8 (14)	123.0	O1-C8-C7	126.7 (16)	127.0
C1-N1-C10	124.8 (14)	126.3	O1-C8-N1	126.8 (16)	126.4
C6-C1-N1	110.1 (13)	107.9	C10-C9-S1	117.6 (13)	118.8
C2-C1-N1	127.8 (15)	128.6	C14-C9-S1	121.0 (14)	119.2
N1-C10-C11	113.7 (15)	115.2	C8-N1-C1	110.7 (14)	110.4
N2-C7-C8	127.7 (14)	126.3	C8-N1-C15	123.5 (15)	122.9
N2-C7-C6	125.9 (15)	126.8	C7-N2-N3	116.2 (14)	117.8
			N2-N3-S1	118.5 (12)	118.9
			N3-S1-C9	105.4 (8)	104.0
			O2-S1-C9	107.8 (8)	107.1
			O2-S1-N3	103.3 (8)	108.7
			O3-S1-C9	107.9 (8)	108.7
			O3-S1-N3	109.6 (8)	102.9
			O3-S1-O2	121.5 (9)	123.5

Table 5: In vitro urease inhibition results of **4** and **5**

Compound		**R**	**Yield (%)**	**Inhibition (%) at 0.5 mM**	**IC_{50} (µM)**
4	CH_2=CH-CH_2	CH_3	80	92.75±0.22	15.26±0.16
5	CH_2=CH-CH_2	3-NO_2Ph	83	75.44±0.23	58.78±0.12
Standard Thiourea				98.45±0.87	21.25±0.15